

Centralized and decentralized control of structural vibration and sound radiation

Wouter P. Engels,^{a)} Oliver N. Baumann, and Stephen J. Elliott
*Institute of Sound and Vibration Research, University of Southampton, University Road, Highfield,
Southampton, SO17 1BJ, United Kingdom*

R. Fraanje
Delft Center for Systems and Control, Delft University, Mekelweg 2, 2628 CD, Delft, The Netherlands

(Received 23 March 2005; revised 15 November 2005; accepted 11 December 2005)

This paper examines the performance of centralized and decentralized feedback controllers on a plate with multiple colocated velocity sensors and force actuators. The performance is measured by the reduction in either kinetic energy or sound radiation, when the plate is excited with a randomly distributed, white pressure field or colored noise. The trade-off between performance and control effort is examined for each case. The controllers examined are decentralized absolute velocity feedback, centralized absolute velocity feedback control and linear quadratic Gaussian (LQG) control. It is seen that, despite the fact that LQG control is a centralized, dynamic controller, there is little overall performance improvement in comparison to decentralized direct velocity feedback control if both are limited to the same control effort. © 2006 Acoustical Society of America.
[DOI: 10.1121/1.2163270]

PACS number(s): 43.40.Vn [KAC]

Pages: 1–XXXX

I. INTRODUCTION

Various control strategies can be used to control the vibration of plates. They can be aimed specifically at controlling the kinetic energy of the plate (active vibration control, AVC) or the sound radiation (active structural acoustic control, ASAC). If a reference signal is not available, control strategies are limited to the use of feedback controllers. These can vary greatly in complexity. The complexity of the controller is understood here to be determined by both the number of states in the controller and whether the controller is centralized or decentralized.

Decentralized, static gain control is the simplest form of feedback control. If it is applied in a stable system where the sensors and actuators are colocated and dual, then stability is, in theory, guaranteed [Balas (1979), Sun (1996)]. In a practical situation, it can have the extra advantage that no connections are required between different control locations and/or a central processing unit and that actuator, sensor and controller could be produced as identical modular units. Decentralized feedback control has been examined by, amongst others Elliott *et al.* (2002), who compare the performance using colocated force actuators and velocity sensors with piezoelectric actuators and velocity sensors. Gardonio *et al.* (2004) gives an extensive review of control methods in ASAC as well as examining the total sound radiation of a panel as a function of a centrally set feedback gain for 16 control loops consisting of piezoceramic patches as actuators and accelerometers as sensors. This means that sensor and actuator are not dual and the stability of the feedback loop is limited. Also, by limiting the system to have the same gain in each control loop, the feedback gains are not optimal. Engels

et al. (2004) compares centralized and decentralized, constant gain control on a beam, but does not take the control effort into account.

More complex controllers have also been examined. Fuller *et al.* (2004) describes heterogeneous blankets for AVC and ASAC, that essentially consist of numerous mass-spring resonators. These resonators could be viewed as decentralized, colocated, dynamic feedback loops. Bingham *et al.* (2001) examines different strategies in several single-input–single-output loops applied to the same plate and found that more complex strategies do result in better performance, but the control loops were not dual, nor was control effort examined. Clark and Cox (1997) compares LQG control and a centralized constant gain controller, optimized for ASAC on a plate with dual control loops and showed that constant gain, velocity feedback can be an effective alternative for dynamic controllers. Though the control effort weighting was the same in the cost function minimized by both control strategies, the actual effort may still have been considerably different. Following-up on this work, Smith and Clark (1998) compared the acoustic performance of static feedback gains in different controller arrangements. Each controller was used to minimize specific cost functions, but now the control effort weighting was adjusted such that the different controllers used the same control effort. For a single channel controller, LQG control and static feedback control were also compared. It was shown that designing for ASAC did result in slightly improved sound reductions for all controllers and that, for a single channel case with a large, distributed sensor/actuator, LQG control gave better performance than static feedback control. However, the complexity of the LQG controller makes it considerably more difficult to implement.

^{a)}Electronic mail: we@isvr.soton.ac.uk

TABLE I. Variables of the plate used in the simulations.

$E=7 \times 10^{10}$ (Pa)	$\rho=2720$ (kg/m ³)
$\zeta=0.01$	$h=0.001$ (m)
$l_x=0.247$ (m)	$l_y=0.278$ (m)
$f_{\max}=3$ (kHz)	$I=h^3/12$ (m ³)

To select an appropriate degree of complexity for the controller, the performance of the different strategies needs to be compared on an even footing. In particular, the control effort that is applied by the controller must be taken into account, as optimization of the cost function for different controllers tends to result in different control efforts. It is also important to examine the trade-off between performance and control effort for different controller designs to select an appropriate amount of control effort. This paper will compare the performance and control effort for a decentralized constant gain controller, a centralized constant gain controller and a centralized linear quadratic Gaussian (LQG) controller. The controllers will be optimized for different performance measures and different excitation spectra of a simply supported plate. The different performance measures are the kinetic energy of the plate or the sound power radiated into the far field. The parameters of the plate used in the study are listed in Table I and it is assumed to be excited by a spatially completely random pressure field with a spectrum corresponding to white noise. This is an idealization of a turbulent boundary layer excitation, as in reality the spatial correlation of turbulent boundary layer has some finite value [Maury *et al.* (2002)]. Colored noise is also examined. Sixteen equally spaced, colocated actuators and sensors are assumed to be arranged on the plate, as shown in Fig. 1. The actuators are assumed to be ideal point force actuators and the sensors ideal velocity sensors.

II. STRUCTURAL MODEL

The model of the simply supported plate, consists of a modal model as described in Fuller *et al.*(1996). The mode shapes are defined as

$$\Psi_{mn}(x,y) = \sin(k_mx)\sin(k_ny) \quad (1)$$

with $k_m=m\pi/l_x$ and $k_n=n\pi/l_y$. The natural frequency corresponding to the above mode is

$$\omega_{mn} = \sqrt{(EI/\rho h)(k_m^2 + k_n^2)}. \quad (2)$$

A small amount of damping, ζ is included in the response of the modes. The response of the amplitude of each mode, a_{mn} , to a harmonic point force, $F_\omega(j\omega)$, acting at a point (x,y) on the plate then is

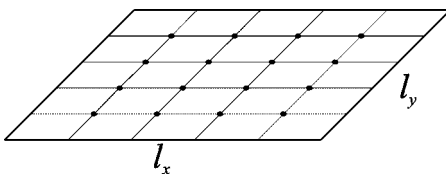


FIG. 1. Equally spaced sensors and actuators. Each dot represents colocated velocity sensors and point force actuator pair.

$$a_{mn}(j\omega) = \frac{4\Psi_{mn}(x,y)F_\omega(j\omega)}{M(\omega_{mn}^2 + 2j\zeta\omega\omega_{mn} - \omega^2)}, \quad (3)$$

where M is the total mass of the plate. If only a finite number, N , of modes is taken into account and the total response of the system can be written in a state space model,

$$\begin{pmatrix} \dot{\mathbf{a}}_s \\ \ddot{\mathbf{a}}_s \end{pmatrix} = \begin{bmatrix} \mathbf{0} & \mathbf{I} \\ -\mathbf{K}_s & -\mathbf{D}_s \end{bmatrix} \begin{pmatrix} \mathbf{a}_s \\ \dot{\mathbf{a}}_s \end{pmatrix} + \frac{4}{M} \begin{pmatrix} \mathbf{0} \\ \Psi \end{pmatrix} \mathbf{F}_t(t), \quad (4)$$

where \mathbf{a}_s and $\dot{\mathbf{a}}_s$ are, respectively, vectors of the modal amplitude and modal velocity. The mode shapes taken into account are all the mode shapes with a natural frequency up to f_{\max} , which results in 60 modes taken into account. The matrix \mathbf{K}_s is a matrix with the squared natural frequencies, ω_{mn}^2 , on its diagonal and empty otherwise. The matrix \mathbf{D}_s is also a diagonal matrix, but with the damping terms of the denominator of Eq. (3), $2\zeta\omega_{mn}$ on its diagonal.

For the chosen mode shapes, the kinetic energy of the plate at any particular point in time, can be calculated as the sum of the squared modal velocities [Meirovitch (1986)]

$$J_{ke} = \frac{M}{8} \dot{\mathbf{a}}_s^T(t) \dot{\mathbf{a}}_s(t). \quad (5)$$

III. RADIATION MODEL

The modeling of sound radiation of a plate in an infinite baffle is usually done in one of two ways, either by analyzing modal radiation or the so-called radiation modes. Modal radiation models the autoradiation and cross radiation of the structural modes and has been used in several papers [Baumann *et al.* (1991), Thomas and Nelson (1995), Clark and Frampton (1999), Viperman and Clark (1991)] to examine and implement ASAC. The radiation modes are velocity distributions of the structure surface that radiate sound independently and are based on the work by Borgiotti (1990), Elliott and Johnson (1993), and Borgiotti and Jones (1994). These velocity distributions vary with frequency but only slowly so. By assuming that the velocity distributions do not change with frequency, an approximation of the radiated sound power can be obtained. This approach may be called the fixed radiation mode approach [Cox *et al.* (1998), Gibbs *et al.* (2000), Gardonio and Elliott (2004)]. Gibbs *et al.* (2000) called this method radiation modal expansion (RME). Though this approach is limited in the frequency range for which it can accurately model the sound radiation, it requires far less states than the full modal radiation approach, used by Baumann *et al.* (1991), as for RME the required number of filters is equal to the number of radiation modes, rather than proportional to the square of the number of structural modes for the modal radiation approach.

In RME, a set of the most significantly radiating modes is chosen at a specific base frequency. Then, the radiated sound power of these modes is calculated at other frequencies and filters are fitted whose squared response matches these values. By calculating the input to each radiation mode as a function of the modal velocities and then applying the frequency dependent filters, the sound radiation J_{ac} can be estimated as

$$\dot{\mathbf{a}}_{ac} = \mathbf{A}_{ac}\mathbf{a}_{ac} + \mathbf{B}_{ac}\dot{\mathbf{a}}_s,$$

$$\mathbf{q} = \mathbf{C}_{ac}\mathbf{a}_{ac} + \mathbf{D}_{ac}\dot{\mathbf{a}}_s,$$

$$J_{ac} = \mathbf{q}^T(t)\mathbf{q}(t), \quad (6)$$

where \mathbf{a}_{ac} are the states of the radiation filters, the matrix \mathbf{B}_{ac} describes the excitation of the filters as a function of the modal velocities, and \mathbf{A}_{ac} describes the dynamics. \mathbf{C}_{ac} describes the relation between the states of each filter and its output and \mathbf{D}_{ac} is a direct feedthrough matrix of the structural velocities to the cost variables.

Here, the 20 most significant radiation modes of the plate at 1 kHz have been selected to model the radiation. The inclusion of these filters in the state space model of Eq. (4) leads to a modified state space model,

$$\begin{pmatrix} \dot{\mathbf{a}}_s \\ \dot{\mathbf{a}}_s \\ \dot{\mathbf{a}}_{ac} \end{pmatrix} = \begin{bmatrix} \mathbf{0} & \mathbf{I} & \mathbf{0} \\ -\mathbf{K}_s & -\mathbf{D}_s & \mathbf{0} \\ \mathbf{0} & \mathbf{B}_{ac} & \mathbf{A}_{ac} \end{bmatrix} \begin{pmatrix} \mathbf{a}_s \\ \dot{\mathbf{a}}_s \\ \mathbf{a}_{ac} \end{pmatrix} + \frac{4}{M} \begin{pmatrix} \mathbf{0} \\ \mathbf{\Psi} \\ \mathbf{0} \end{pmatrix} \mathbf{F}_t(t),$$

$$\mathbf{q} = [\mathbf{0} \ \mathbf{D}_{ac} \ \mathbf{C}_{ac}] \begin{pmatrix} \mathbf{a}_s \\ \dot{\mathbf{a}}_s \\ \mathbf{a}_{ac} \end{pmatrix}. \quad (7)$$

IV. COST FUNCTION FORMULATION

The two goals of control are to minimize the kinetic energy of the system or the radiated sound power. Also, the control effort used to control the system should be limited. The excitation of the system is assumed to be a random signal in the time domain. Hence, the cost function is chosen to be the time average or expectation, of the two values mentioned above and the control effort, thus resulting in the following expressions for the cost functions relating to kinetic energy, J_{ke} , and sound radiation, J_{ac} , respectively,

$$J_{ke} = E[M/8\dot{\mathbf{a}}_s^T(t)\dot{\mathbf{a}}_s(t) + \rho\mathbf{u}^T(t)\mathbf{u}(t)], \quad (8)$$

$$J_{ac} = E[\mathbf{q}^T(t)\mathbf{q}(t) + \rho\mathbf{u}^T(t)\mathbf{u}(t)], \quad (9)$$

where \mathbf{u} is the vector of control signals applied by the controller and ρ is a weighting value of the control effort. To compare the controllers fairly, ρ should be tuned such that the control effort $\mathbf{u}^T(t)\mathbf{u}(t)$ is equal for each controller. Because the variables in the above equations are all dependent on the random excitation of the system, it is useful to rewrite them in terms of the expectation of the excitation.

Both of the above equations can be written in a more general form,

$$J = E[\mathbf{x}^T(t)\mathbf{Q}\mathbf{x}(t) + \mathbf{u}^T(t)\mathbf{R}\mathbf{u}(t)], \quad (10)$$

where \mathbf{x} are the states of the model, in this case, \mathbf{a}_s , $\dot{\mathbf{a}}_s$ and, if needed, \mathbf{a}_{ac} . Equations (4) and (7) can then be written in a general state-space form:

$$\dot{\mathbf{x}}(t) = \mathbf{A}\mathbf{x}(t) + \mathbf{B}_u\mathbf{u}(t) + \mathbf{B}_d\mathbf{F}_t(t), \quad (11)$$

$$\mathbf{y}(t) = \mathbf{C}\mathbf{x}(t),$$

where the forcing term $\mathbf{F}_t(t)$ has been split into a disturbance force \mathbf{F}_d and a control force \mathbf{u} . The matrices \mathbf{B}_d and \mathbf{B}_u are structured in the same way as the matrix preceding the forcing term \mathbf{F}_t in Eqs. (4) and (7).

If a feedback controller is used, the feedback gain is a function of the states of the system and the states of the controller. The terms $\mathbf{u}(t)\mathbf{R}\mathbf{u}(t)$ and $\mathbf{B}_u\mathbf{u}(t)$ can then be removed from Eqs. (10) and (11) without loss of generality, by including the controller in the states $\mathbf{x}(t)$ and the matrix \mathbf{A} . The cost of the control effort can then be included in the term $\mathbf{x}^T(t)\mathbf{Q}\mathbf{x}(t)$. To distinguish between the dynamics of the controlled and uncontrolled system, the notation \mathbf{A}_c is used for the controlled system.

The states at any particular time are a convolution of the matrix of impulse responses of the states to a change in any of the states and the excitation of the modes by the disturbance,

$$\mathbf{x}(t) = \mathbf{\Phi}(t) * \mathbf{B}_d\mathbf{F}_t(t), \quad (12)$$

where $\mathbf{\Phi}(t)$ is the matrix of the impulse responses of the states. This matrix is also known as the *fundamental transition matrix* and is equal to

$$\mathbf{\Phi}(t) = e^{\mathbf{A}_c t}. \quad (13)$$

Combining Eqs. (10) and (12) and including control effort in the matrix \mathbf{Q} , results in

$$\begin{aligned} J &= E[\mathbf{x}^T(t)\mathbf{Q}\mathbf{x}(t)] = \text{trace}(\mathbf{Q}E[\mathbf{x}(t)\mathbf{x}^T(t)]) \\ &= \text{trace}(\mathbf{Q}E[\mathbf{\Phi}(t) * \mathbf{B}_d\mathbf{F}_t(t)(\mathbf{\Phi}(t) * \mathbf{B}_d\mathbf{F}_t(t))^T]) \\ &= \text{trace}\left(\mathbf{Q}E\left[\int_0^\infty \mathbf{\Phi}(\sigma_1)\mathbf{B}_d\mathbf{F}_t(t-\sigma_1)d\sigma_1 \right. \right. \\ &\quad \left. \left. \times \int_0^\infty \mathbf{F}_t^T(t-\sigma_2)\mathbf{B}_d^T\mathbf{\Phi}^T(\sigma_2)d\sigma_2\right]\right) \\ &= \text{trace}\left(\mathbf{Q}\int_0^\infty \int_0^\infty \mathbf{\Phi}(\sigma_1)\mathbf{B}_dE[\mathbf{F}_t(t-\sigma_1) \right. \\ &\quad \left. \times \mathbf{F}_t^T(t-\sigma_2)]\mathbf{B}_d^T\mathbf{\Phi}^T(\sigma_2)d\sigma_1 d\sigma_2\right). \end{aligned} \quad (14)$$

Expectation $E[\mathbf{F}_t(t-\sigma_1)\mathbf{F}_t^T(t-\sigma_2)]$ contains the correlations in time between the disturbing forces. If these forces are mutually uncorrelated, the matrix is diagonal. If the signals are uncorrelated in time, the matrix is only nonzero if $\sigma_1 = \sigma_2$, in which case, the expectation is a constant matrix, $\mathbf{E}_{\mathbf{F}\mathbf{F}^T}$, and Eq. (14) simplifies considerably,

$$J = \text{trace} \left(\mathbf{Q} \int_0^\infty \Phi(\sigma) \mathbf{B}_d \mathbf{E}_{\text{FF}} \mathbf{B}_d^T \Phi^T(\sigma) d\sigma \right) \quad (15)$$

or

$$J = \text{trace} \left(\int_0^\infty \Phi^T(\sigma) \mathbf{Q} \Phi(\sigma) d\sigma \mathbf{B}_d \mathbf{E}_{\text{FF}} \mathbf{B}_d^T \right). \quad (16)$$

No specific assumptions have so far been made on the location of the excitation. As can be seen from Eq. (3), the location would influence the matrix \mathbf{B}_d and thus also the cost functions. In this analysis, the influence of the location of the excitation is an undesirable complication. If it is assumed that the excitation is a spatially completely random pressure field, this is equivalent to assuming that all the modes of the structure are excited equally, but in an uncorrelated fashion. This can be shown by analyzing the correlation between the excitation of the different modes.

Equation (4) describes how the modes are excited by point forces. Consider now the excitation of a single mode mn , $f_{mn}(t)$, by a pressure field, $p(x, y)$,

$$f_{mn}(t) = \frac{4}{M} \int_0^{l_y} \int_0^{l_x} \Psi_{mn}(x, y) p(x, y, t) dx dy. \quad (17)$$

The correlation between a mode kl and mode mn would then be, at any point in time

$$\begin{aligned} E[f_{kl} f_{mn}] &= \frac{16}{M^2} E \left[\int_0^{l_y} \int_0^{l_x} \Psi_{kl}(x_1, y_1) p(x_1, y_1, t) dx_1 dy_1 \right. \\ &\quad \left. \times \int_0^{l_y} \int_0^{l_x} \Psi_{mn}(x_2, y_2) p(x_2, y_2, t) dx_2 dy_2 \right] \\ &= \frac{16}{M^2} \int_0^{l_y} \int_0^{l_x} \int_0^{l_y} \int_0^{l_x} \Psi_{kl}(x_1, y_1) \Psi_{mn}(x_2, y_2) \\ &\quad \times E[p(x_1, y_1, t) p(x_2, y_2, t)] dx_1 dy_1 dx_2 dy_2. \end{aligned} \quad (18)$$

For a spatially completely random pressure field, there is no correlation between the pressures at two different locations and $E[p(x_1, y_1, t) p(x_2, y_2, t)]$ is equal to $\delta(x_1 - x_2) \delta(y_1 - y_2) E[p(x_1, y_1, t)^2]$. It is furthermore assumed that $E[p(x, y, t)^2]$ is constant for different (x, y) . Equation (18) can then be rewritten as

$$\begin{aligned} E[f_{kl} f_{mn}] &= \frac{16}{M^2} \int_0^{l_y} \int_0^{l_x} \Psi_{kl}(x, y) \Psi_{mn}(x, y) E[p(x, y, t)^2] dx dy \\ &= \frac{16}{M^2} \int_0^{l_y} \int_0^{l_x} \Psi_{kl}(x, y) \Psi_{mn}(x, y) dx dy E[p(x, y, t)^2]. \end{aligned} \quad (19)$$

For the assumed, orthogonal mode shapes, the integral $\int_0^{l_y} \int_0^{l_x} \Psi_{kl}(x, y) \Psi_{mn}(x, y) dx dy$ is nonzero only if $kl = mn$, when it is equal to $l_x l_y / 4$.

If the pressure field is assumed to have a white spectrum in time, as well as space, then Eqs. (19) and (16) can be combined,

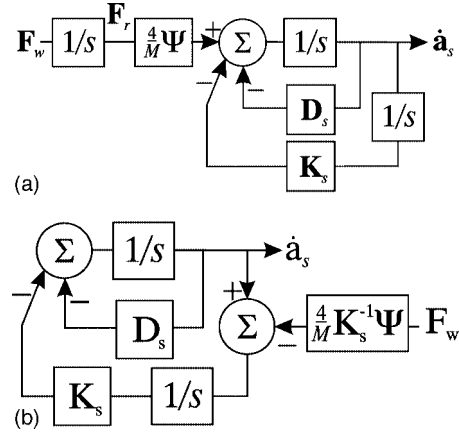


FIG. 2. Equivalent ways of modeling red noise, if velocity sensors and velocity based cost functions are used.

$$J = \text{trace} \left(\int_0^\infty \Phi^T(\sigma) \mathbf{Q} \Phi(\sigma) d\sigma \mathbf{P}_w \right) \quad (20)$$

with

$$\mathbf{P}_w = \left(\frac{4}{M} \right)^2 \begin{bmatrix} \mathbf{0} & \mathbf{0} \\ \mathbf{0} & \mathbf{I} \end{bmatrix}. \quad (21)$$

Here, the magnitude of the expectation $E[p(x, y, t)^2]$ is chosen to be equal to $4/l_x l_y [N^2/m^4]$ and $\Phi(t)$ was assumed to only describe the structural states, with the state space vector $\mathbf{x} = [\mathbf{a}_s^T \mathbf{a}_s^T]^T$. With this model, each of the structural modes is excited and also taken into account in the cost function. If acoustic radiation is examined, the matrix \mathbf{P}_w needs to be extended with zeros for the states of the acoustic filters. The same should be done for the states of the controller if a dynamic velocity feedback controller is included in the states of the system. Spatially and temporally uncorrelated excitation can be used as a model for a turbulent boundary layer excitation.

To model nonwhite noise, generally, extra states should be added to the system to color the noise before it acts on the system. However, for red noise, i.e., integrated white noise, in a system using velocity sensors and a velocity dependent cost function it can be shown that the shaping of the white noise can also be done without adding extra states, as can be seen from Figs. 2(a) and 2(b). The following matrix can then be used to calculate the red noise excitation,

$$\mathbf{P}_r = \left(\frac{4}{M} \right)^2 \begin{bmatrix} (\mathbf{K}_s^{-1})^T \mathbf{K}_s^{-1} & \mathbf{0} \\ \mathbf{0} & \mathbf{0} \end{bmatrix}, \quad (22)$$

where \mathbf{K}_s is part of the matrix in Eq. (4). This matrix should again be extended with zeros if the acoustic filters or a dynamic controller are taken into account. Note that, though the integrated white noise signal will tend to infinity at low frequencies, the response of the system in terms of modal velocity and radiated sound power, tends to 0. In Sec. V B 1 it is shown that the cost function in Eq. (20) can be evaluated using a solution of a Lyapunov equation as long as the system is asymptotically stable. In that case both cost functions remain bounded.

V. CONTROLLER DESIGN

In addition to the variations in the spectrum of the excitation and cost function, three different controller structures will be examined here; centralized constant gain velocity feedback control, decentralized constant gain velocity feedback control and LQG control. For all three control structures it is assumed that absolute velocity sensors are used with colocated point force actuators. All components are assumed ideal and without time delays.

A. Linear quadratic Gaussian control

An LQG controller [Kalman and Bucy (1961)] consists of two parts. One is the state estimator, which uses measured data to estimate the states of the system under control as accurately as possible. The other part is a feedback gain matrix, with the estimated states as input, and the control signal as outputs. The requirements for the use of LQG control, namely, stabilizability and detectability are met for this problem, as the system under control contains no unstable modes.

The state estimator gives an minimum variance estimation of the states, assuming a white noise excitation acts on the system and an uncorrelated white noise is added to the measured signals. If the excitation is not white noise, extra filters can be added to the model to shape the excitation. However, these filters should then also be included in the state estimation and increase the complexity of the controller.

Under the assumptions set out in Sec. IV for the white, spatially randomly distributed excitation, the matrix needed to calculate the effect of the excitation is the matrix \mathbf{P}_w . The weighting of the sensor noise is chosen to be small compared to the excitation and was set at 1×10^{-4} (m^2/s^2) for each sensor for the white excitation. For red noise, the matrix \mathbf{P}_r has to be used instead of \mathbf{P}_w . Also, the sensor signals are much smaller and to keep the sensor noise small in comparison to the measured signal, the sensor noise is set equal to 1×10^{-10} (m^2/s^2).

The other part of the controller, the feedback gain matrix, would minimize the cost function in Eq. (10) if full state information is available. Further details concerning the design of the LQG controller can be found, for example, in Skogestad and Postlethwaite (1996).

B. Constant gain controllers

When optimizing output feedback controllers, it is difficult to prove that a local minimum of the cost function is also the global minimum. This is discussed by Levine and Athans (1970), who examines constant gain, output feedback specifically. In this paper an algorithm is presented to find a minimum of the cost function, but it is also noted this algorithm is not guaranteed to converge. A different algorithm is used here, which is discussed by Anderson and Moore (1971) and is essentially a gradient descent algorithm. This section describes how this algorithm is implemented for both the centralized and the decentralized constant gain controllers.

1. Centralized constant gain controller

Levine and Athans (1970) examined a general state space model,

$$\dot{\mathbf{x}}(t) = \mathbf{A}\mathbf{x}(t) + \mathbf{B}_u\mathbf{u}(t),$$

$$\mathbf{y}(t) = \mathbf{C}\mathbf{x}(t) \quad (23)$$

with constant output feedback gain

$$\mathbf{u}(t) = -\mathbf{G}\mathbf{y}(t). \quad (24)$$

A cost function was used, which was similar to the one in Eq. (10). It was noted that, if the system starts at an initial set of states $\mathbf{x}(0)$ and no further external excitation acts on the system, the state at any particular time is given by

$$\mathbf{x}(t) = \Phi(t)\mathbf{x}(0), \quad (25)$$

where $\Phi(t)$ is the fundamental transition matrix for the controlled system, as defined by Eq. (13). For this constant gain output feedback controller, the matrix \mathbf{A}_c is defined as

$$\mathbf{A}_c = \mathbf{A} - \mathbf{B}_u\mathbf{G}\mathbf{C}. \quad (26)$$

Combining Eqs. (25), (24), and (10) results in the equation

$$\begin{aligned} J &= \mathbf{x}^T(0) \int_0^\infty \Phi^T(t) [\mathbf{Q} + \mathbf{C}^T\mathbf{G}^T\mathbf{R}\mathbf{G}\mathbf{C}] \Phi(t) dt \mathbf{x}(0) \\ &= \text{trace} \left(\int_0^\infty \Phi^T(t) [\mathbf{Q} + \mathbf{C}^T\mathbf{G}^T\mathbf{R}\mathbf{G}\mathbf{C}] \Phi(t) dt \mathbf{x}(0)\mathbf{x}^T(0) \right). \end{aligned} \quad (27)$$

It can be easily seen that this is similar to Eq. (20), if $\mathbf{x}(0)\mathbf{x}^T(0)$ is replaced by \mathbf{P}_w . \mathbf{P}_r is used when studying red noise excitation. If the system is asymptotically stable and the matrix \mathbf{Q} is positive semidefinite, the cost function is bounded and equal to [Kalman and Bertram (1960)]

$$J = \text{trace}(\mathbf{K}\mathbf{P}_w) \quad (28)$$

with \mathbf{K} the positive definite solution of the Lyapunov equation

$$\begin{aligned} \mathbf{K}[\mathbf{A} - \mathbf{B}_u\mathbf{G}\mathbf{C}] + [\mathbf{A} - \mathbf{B}_u\mathbf{G}\mathbf{C}]^T\mathbf{K} + [\mathbf{Q} + \mathbf{C}^T\mathbf{G}^T\mathbf{R}\mathbf{G}\mathbf{C}] \\ = \mathbf{0}. \end{aligned} \quad (29)$$

The derivative of the cost function, J , with respect to the elements of the feedback gain matrix, \mathbf{G} , is equal to

$$\frac{\partial J}{\partial \mathbf{G}} = 2\mathbf{R}\mathbf{G}\mathbf{C}\mathbf{L}\mathbf{C}^T = 2\mathbf{B}_u^T\mathbf{K}\mathbf{L}\mathbf{C}^T, \quad (30)$$

where \mathbf{K} is the solution of Eq. (29) and \mathbf{L} is the solution of

$$[\mathbf{A} - \mathbf{B}_u\mathbf{G}\mathbf{C}]\mathbf{L} + \mathbf{L}[\mathbf{A} - \mathbf{B}_u\mathbf{G}\mathbf{C}]^T + \mathbf{P}_w = \mathbf{0}. \quad (31)$$

Using the derivative of the feedback gain, a simple algorithm can be formulated that will converge to a minimum on the cost function, if started at an initial stabilizing controller \mathbf{G}_0 . The algorithm used here is similar to that in Anderson and Moore (1971):

- (i) Calculate the cost J_k using Eqs. (28) and (29). If $k = 0$, use the initial stabilizing controller \mathbf{G}_0 .

- (ii) Calculate the derivative of the cost function $\partial J_k / \partial \mathbf{G}_k$, using Eq. (30).
- (iii) Update the gain matrix \mathbf{G}_k according to

$$\mathbf{G}_{k+1} = \mathbf{G}_k - \frac{\epsilon}{\mathbb{F}[\partial J_k / \partial \mathbf{G}_k]} \frac{\partial J_k}{\partial \mathbf{G}_k}, \quad (32)$$

where ϵ is a small value to regulate the stepsize and \mathbb{F} denotes the Frobenius norm. This norm is included to keep the stepsize in G_k independent of the size of the values in $\partial J_k / \partial \mathbf{G}_k$.

- (iv) Check that the system is stable at these new gains and, if that is the case, calculate the cost J_{k+1} . If the system is no longer stable or $J_{k+1} > J_k$, reduce the stepsize ϵ , because the update has overshoot the stability margins or an area where the cost is lower. Repeat the previous step and this step, until the system is stable and $J_{k+1} < J_k$, then repeat from the beginning.
- (v) To stop the optimization, a suitable criterion can be chosen, such as a sufficiently small update in the gains, or a sufficiently small improvement in the cost function.

Though it cannot be proved that the algorithm converges to a global minimum, it is found in practice that the controller does converge to the same set of gains, independent of the choice of initial controller, the only exception is if the control locations are extremely close together [Engels and Elliott (2006)]. Therefore, for ease of formulation, applying the above algorithm will be referred to as *optimization*.

2. Decentralized constant gain controller

Geromel and Bernussou (1979) discussed the optimization of a constant gain decentralized controller, for the same system and cost functions as Levine and Athans (1970). The same algorithm can be used as for centralized control, except that the initial stabilizing control matrix should be diagonal and that the derivative with respect to the elements of the gain matrix is equal to

$$\frac{\partial J}{\partial \mathbf{G}} = \text{diag}[2\mathbf{R}\mathbf{G}\mathbf{C}\mathbf{L}\mathbf{C}^T - 2\mathbf{B}_u^T \mathbf{K}\mathbf{L}\mathbf{C}^T], \quad (33)$$

where diag denotes a function that sets all off-diagonal terms of the matrix to 0.

VI. RESULTS

As noted above, it is important to compare the performance when equal amounts of control effort are used. In this study 16 equally spaced control locations are used, as indicated in Fig. 1. At each control location, ideal velocity sensors are assumed that are colocated with ideal force actuators.

Figures 3(a) and 3(b) show the resulting expectation of the kinetic energy and acoustic radiation when each of the three controllers are optimized for kinetic energy and acoustic radiation, respectively. A white noise excitation is assumed and the control effort weighting was adjusted such that the expected controller effort was equal to $300 N^2$ for each controller. The kinetic energy and sound power density

around the first resonance frequency is reduced by about 25 dB dropping off to about 10 dB reduction at other resonances. Despite the seemingly better performance of LQG control in Fig. 3(a), the integral over time [Eq. (20)] of kinetic energy was reduced by 5.5 dB for *each* of the controllers. For sound power, the reductions were 4.5 dB for LQG control, 4.1 dB for centralized constant gain control, and 4.0 dB for decentralised constant gain control.

Figures 3(c) and 3(d) also show kinetic energy and acoustic radiation, but with a red noise excitation instead of white noise. The level of excitation is far less in this case and so the control effort was now limited to $3 \times 10^{-3} N^2$ for each controller. The reductions in kinetic energy for the different controllers at this effort are 22.3 dB for LQG control and 23.3 dB for both centralized and decentralized constant feedback gain control. For sound power the reductions are, respectively, 19.7, 22.6, and 22.3 dB.

In this case LQG control performs less well than the constant gain controllers. This is due to the extent of the reductions that are achieved, which cause the sensor signals to be in the range of the sensor noise that was assumed in the design of the LQG controller. Though the level of the reductions achieved with this control effort are not obtainable in a real situation due to the presence of sensor noise, the level of control effort was chosen to emphasize the difference between the constant gain and LQG controllers. The reductions that are achieved are much larger than in the white noise case because most of the cost in the cost function is caused by the energy in the first mode.

It is interesting to note that each of the gains in the optimized constant gain decentralized controller were of similar magnitude, but that the optimized centralized constant gain controller also had off-diagonal gains that were of the same order of magnitude as the on-diagonal gains. Despite the magnitude of these gains, they did not contribute significantly to the reduction in the cost function.

The overall difference in the cost function is difficult to see from these plots and it is not clear whether this level of effort is most appropriate. Therefore, the overall reduction in the expected kinetic energy and sound radiation reduction should be examined as a function of control effort. These values can be evaluated using Eqs. (28) and (29). Figure 4(a) and 4(b) show the change in kinetic energy and radiated sound power as a function of the control effort for white noise excitation, which has been computed by optimizing the three controllers with varying control effort weightings. Still higher control efforts can be achieved by using higher gains in the control loops, but this results in worse, rather than better performance. It can be seen that there is some advantage in using LQG control rather than constant gain feedback, since for a given performance, the control effort is slightly lower, but this difference is small. It should be noted that for the control of sound power, the LQG controller requires a total of 347 states.

Figures 4(c) and 4(d) show the results when the system is excited by red noise. There are nearly no differences between the controllers for low control efforts, but the LQG controller performs worse at higher control efforts, which is again due to the fact that the LQG controller takes sensor

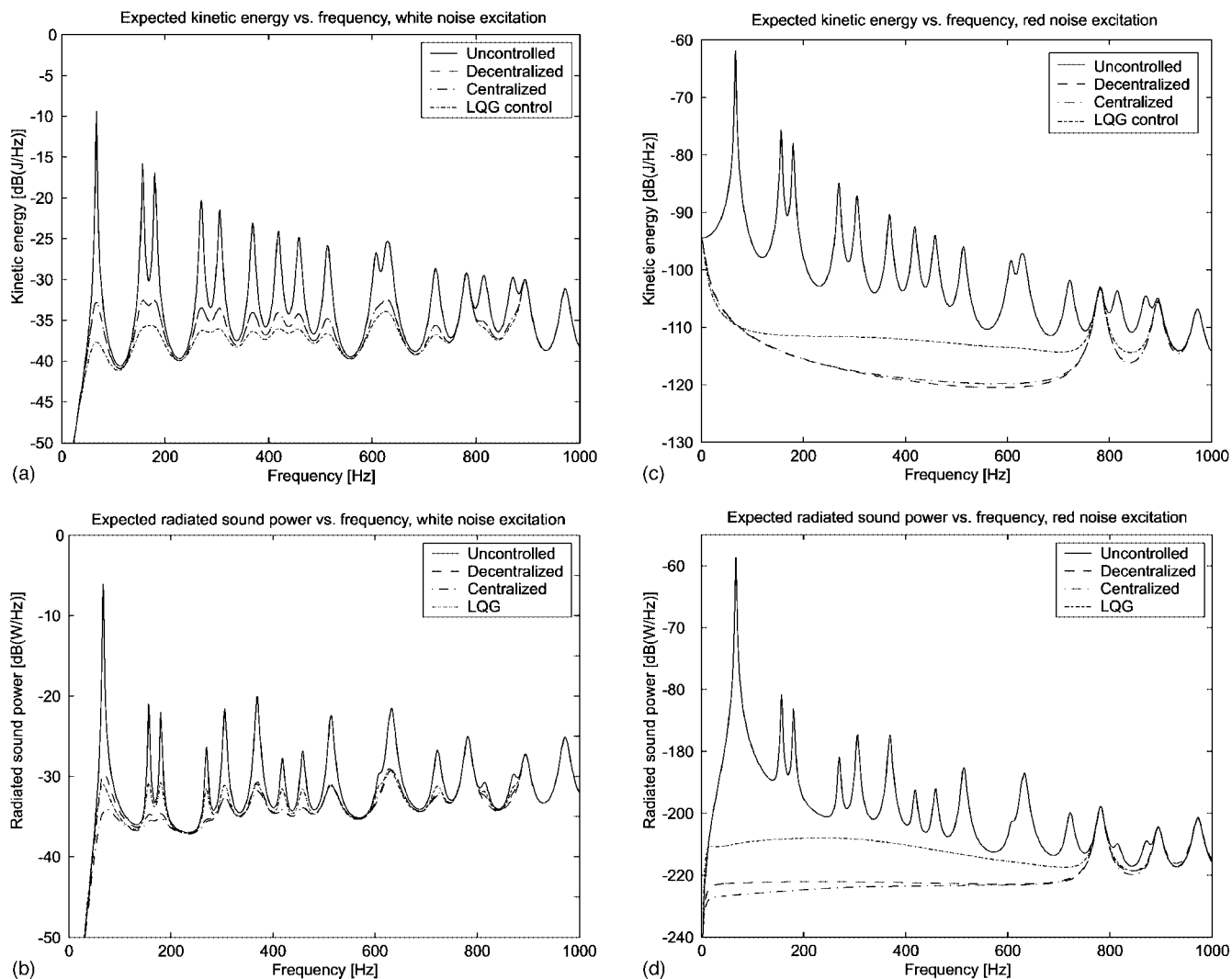


FIG. 3. Spectrum of expected kinetic energy (KE) and radiated sound power (ac), assuming white or red noise excitation, before and after control, using different controllers optimized to control kinetic energy and radiated sound power, respectively. The expected average control effort for each controller was limited to $300 N^2$ for white noise excitation and $3 \times 10^{-3} N^2$ for red noise. (a) KE vs frequency, white noise. (b) ac vs frequency, white noise. (c) KE vs frequency, red noise. (d) ac vs frequency, red noise.

noise into account in the design, but that no noise was taken into account in the calculation of the cost function. These graphs could also provide an important design tool in determining the correct trade off between performance and control effort for a given application.

From these figures it can be seen that there is little difference between the effectiveness of the different controllers. For a white noise excitation there is some advantage in using LQG control over constant gain control if acoustic radiation is considered. However, these results were obtained with the controller at particular points on the plate, where certain modes cannot be controlled, as can be seen in Fig. 3(a). It is not clear how this affects the results obtained and whether the same conclusions can be drawn for a different placement of the actuators. Therefore the difference between the controllers for a given control effort has also been examined for randomly placed control locations. The number of control locations was limited to 5. It was found that the differences between centralized, decentralized constant gain and LQG control remain small, though LQG control did show slightly

better performance in the case of white noise for both kinetic energy and acoustic radiation. LQG control did not improve the performance in the case of red noise excitation, because of the amount of sensor noise considered in the design of the controller.

VII. CONCLUSIONS

For the model problem considered, with 16 collocated velocity sensors and point force actuators, there is little performance gain in using centralized static feedback gain control or LQG control over decentralized static feedback gain control, when similar amounts of control effort are used. LQG control gives some improvement in performance in the case of a white, randomly distributed excitation, but may not be worth the added complexity of the controller. Similar results were also observed for five channel controllers with randomly located control locations.

This seems to contrast with the work of Smith and Clark (1998) who saw a significant improvement at some frequen-

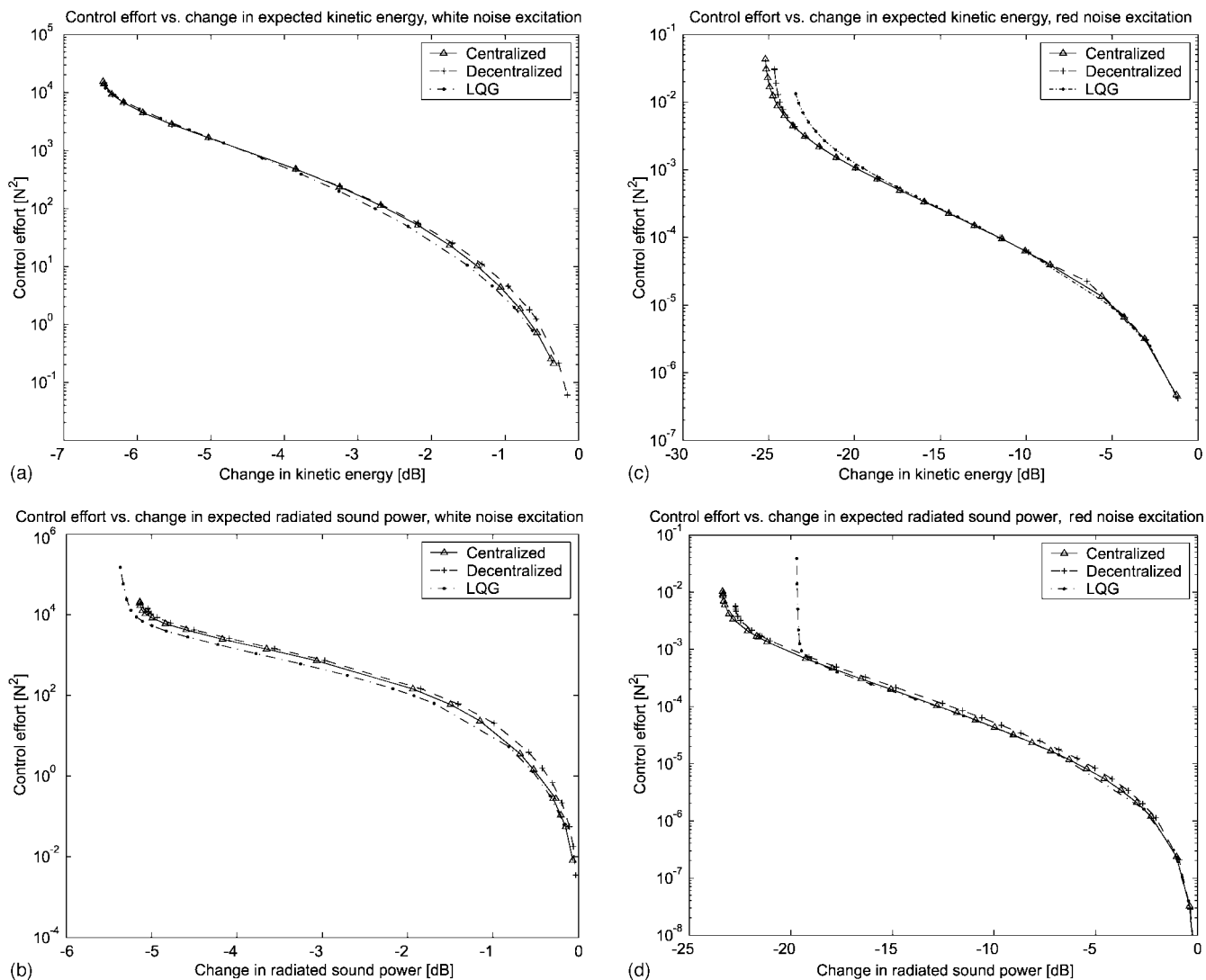


FIG. 4. Change in expected kinetic energy (KE) and radiated sound power (ac) as a function of effort, assuming white or red noise excitation, using different controllers optimized to control kinetic energy and radiated sound power, respectively. (a) KE vs effort, white noise. (b) ac vs effort, white noise. (c) KE vs effort, red noise. (d) ac vs effort, red noise.

cies, when using LQG control in a single channel controller and a large distributed sensoriactuator. The frequency range over which this improvement occurred was limited though and results, on average, in only a small difference. Elliott (2004) has noted that if the number of control loops is equal to the number of controlled modes, then under idealized circumstances the effect of a decentralized constant gain controller would be equal to that of a fully coupled modal controller. Although in these simulations, 60 structural modes were taken into account in both the model and the cost function, the total kinetic energy is dominated by a significantly smaller number of modes, as can be seen from Fig. 3(a) for white noise excitation, and an even smaller number for red noise excitation, Fig. 3(c). This may explain why, in the case of red noise excitation, when there are only very few modes contributing significantly to the cost function, there is hardly any difference between centralized, decentralized, and LQG control. Further research into the relation between the number of excited modes and the number of control locations for which the difference in performance between dynamic controllers and static controllers becomes small, may prove in-

teresting. Using piezoceramic actuators can be more practical than a point force actuator and it would be interesting to see if the use decentralized, constant gain control is as effective in that case as here. The stability of constant gain feedback controllers using such actuators does require careful attention [Gardonio and Elliott (2004)].

ACKNOWLEDGMENTS

This work has been partly funded by the European Community InMAR project and partly by the Engineering and Physical Sciences Research Council (EPSRC). The work of one of the authors (O.B.) is sponsored by the Data Information Fusion Defence Technology Centre. Furthermore, the authors would like to thank Michel Verhaegen for useful discussions on this topic.

Anderson, B. D. O., and Moore, J. B. (1971). *Linear Optimal Control* (Prentice-Hall, Englewood Cliffs, NJ).
 Balas, M. J. (1979). "Direct velocity feedback control of large space structures." *J. Guid. Control* **2**, 252–253.
 Baumann, W. T., Saunders, W. R., and Robertshaw, H. H. (1991). "Active

- suppression of acoustic radiation from impulsively excited structures," *J. Acoust. Soc. Am.* **90**, 3202–3206.
- Bingham, B., Atalla, M. J., and Hagood, N. W. (2001). "Comparison of structural-acoustic designs on an active composite panel," *J. Sound Vib.* **244**, 761–778.
- Borgiotti, G. V. (1990). "The power radiated by a vibrating body in an acoustic fluid and its determination from boundary measurements," *J. Acoust. Soc. Am.* **88**, 1884–1893.
- Borgiotti, G. V., and Jones, K. E. (1994). "Frequency independence property of radiation spatial filters," *J. Acoust. Soc. Am.* **96**, 3516–3524.
- Clark, R. L., and Cox, D. E. (1997). "Multi-variable structural acoustic control with static compensation," *J. Acoust. Soc. Am.* **102**, 2747–2756.
- Clark, R. L., and Frampton, K. D. (1999). "Aeroelastic structural acoustic control," *J. Acoust. Soc. Am.* **102**, 743–754.
- Cox, D. E., Gibbs, G. P., Clark, R. L., and Vipperman, J. S. (1998). "Experimental robust control of structural acoustic radiation," *39th AIAA/ASME/ASCE/AHS/ASC Structures, Structural Dynamics and Materials Conference (AIAA)*.
- Elliott, S. J. (2004). "Distributed control of sound and vibration," *Proceedings of ACTIVE04*.
- Elliott, S. J., Gardonio, P., Sors, T. C., and Brennan, M. J. (2002). "Active vibroacoustic control with multiple local feedback loops," *J. Acoust. Soc. Am.* **111**, 908–915.
- Elliott, S. J., and Johnson, M. E. (1993). "Radiation modes and the active control of sound power," *J. Acoust. Soc. Am.* **94**, 2194–2204.
- Engels, W. P., Baumann, O. N., and Elliott, S. J. (2004). "Centralized and decentralized feedback control of kinetic energy," *Proceedings of ACTIVE04*.
- Engels, W. P., and Elliott, S. J. (2006). Optimal velocity feedback control on a beam (unpublished).
- Fuller, C. R., Elliott, S. J., and Nelson, P. A. (1996). *Active Control of Vibration* (Academic, London).
- Fuller, C. R., Kidner, M., Li, X., and Hansen, C. H. (2004). "Active-passive heterogeneous blankets for control of vibration and sound radiation," *Proceedings of ACTIVE04*.
- Gardonio, P., Bianchi, E., and Elliott, S. (2004). "Smart panel with multiple decentralized units for the control of sound transmission. Part I: theoretical predictions," *J. Sound Vib.* **274**, 163–192.
- Gardonio, P., and Elliott, S. (2004). "Smart panels for active structural acoustic control," *Smart Mater. Struct.* **13**, 1314–1336.
- Geromel, J. C., and Bernussou, J. (1979). "An algorithm for optimal decentralized regulation of linear quadratic interconnected systems," *Automatica* **15**, 489–491.
- Gibbs, G. P., Clark, R. L., Cox, D. E., and Vipperman, J. S. (2000). "Radiation modal expansion: Application to active structural acoustic control," *J. Acoust. Soc. Am.* **107**, 332–339.
- Kalman, R. E., and Bertram, J. E. (1960). "Control system analysis and design via the "second method" of Lyapunov, I Continuous-time systems," *J. Basic Eng.* **82**, 371–393.
- Kalman, R. E., and Bucy, R. S. (1961). "New results in linear filtering and prediction theory," *J. Basic Eng.* **83**, 95–108.
- Levine, W. S., and Athans, M. (1970). "On the determination of the optimal constant output feedback gains for linear multivariable systems," *IEEE Trans. Autom. Control* **AC-15**, 44–48.
- Maury, C., Gardonio, P., and Elliott, S. J. (2002). "A wavenumber approach to modeling the response of a randomly excited panel, part I: general theory," *J. Sound Vib.* **252**, 83–113.
- Meirovitch, L. (1986). *Elements of Vibration Analysis*, 2nd ed. (McGraw-Hill, New York).
- Skogestad, S., and Postlethwaite, I. (1996). *Multivariable Feedback Control—Analysis and Design* (Wiley, Chichester, England).
- Smith, G. C., and Clark, R. L. (1998). "The influence of frequency-shaped cost functionals on the structural acoustic control performance of static, output feedback controllers," *J. Acoust. Soc. Am.* **104**, 2236–2244.
- Sun, J. Q. (1996). "Some observations on physical duality and colocation of structural control sensors and actuators," *J. Sound Vib.* **194**, 765–770.
- Thomas, D. R., and Nelson, P. A. (1995). "Feedback control of sound radiation from a plate excited by a turbulent boundary layer," *J. Acoust. Soc. Am.* **98**, 2561–2662.
- Vipperman, J. S., and Clark, R. (1991). "Implications of using collocated strain-based transducers for output active structural acoustic control," *J. Acoust. Soc. Am.* **106**, 1392–1399.